

Virtual tryout planning in automotive industry based on simulation metamodels

D Harsch¹, J Heingärtner¹, D Hortig² and P Hora³

¹ inspire AG - ivp, Technoparkstrasse 1, 8005 Zürich, Switzerland

² Daimler AG, Käsbrunnlestrasse, 71059 Sindelfingen, Germany

³ ETH Zürich, Institute of Virtual Manufacturing,
Tannenstr. 3, 8092 Zürich, Switzerland

E-mail: harsch@inspire.ethz.ch

Abstract. Deep drawn sheet metal parts are increasingly designed to the feasibility limit, thus achieving a robust manufacturing is often challenging. The fluctuation of process and material properties often lead to robustness problems. Therefore, numerical simulations are used to detect the critical regions. To enhance the agreement with the real process conditions, the material data are acquired through a variety of experiments. Furthermore, the force distribution is taken into account. The simulation metamodel contains the virtual knowledge of a particular forming process, which is determined based on a series of finite element simulations with variable input parameters. Based on the metamodels, virtual process windows can be displayed for different configurations. This helps to improve the operating point as well as to adjust process settings in case the process becomes unstable. Furthermore, the time of tool tryout can be shortened due to transfer of the virtual knowledge contained in the metamodels on the optimisation of the drawbeads. This allows the tool manufacturer to focus on the essential, to save time and to recognize complex relationships.

1. Introduction

Given the increasingly tighter tolerance requirements, the fluctuation of process and material properties, as well as changing environmental conditions, often lead to robustness problems during series production [1][2]. In the current state of the art the factors influencing robustness are not systematically measured and online action is limited to a manual intervention on a trial-and-error basis. The quality of the outcome is thus strongly correlated to the experience of the staff and eventual corrections are costly. Additional circumstances, such as the reduction of the material thickness, complex geometries with sharp radii and the flexible choice of the press, limit the process stability even further.

In order to increase the significance and illustration accuracy of the simulations, a variety of different arrangements are taken into account, such as the use of accurate material models based on experiments, the consideration of the press construction and the implementation of digitised tool geometries. The goal of the project is to inspect the critical regions at an early stage regarding robustness problems and to propose improvement measures. Furthermore, the virtual knowledge of the simulation should be transferred to the tool tryout in order to support the staff with purposeful actions. In this work, a methodological approach based on simulation metamodels is developed to find a suitable operating point and to generate virtual tryout maps around the operating point. Thus, cost-intensive rework could be reduced or even avoided.



2. Process description

The trunk lid of the actual B-class by Daimler shows diverse imperfections during serial pressing, such as splits, wrinkling, hardening through minimal thinning, sink marks and skid impact lines. The simulations in the planning stage did not class all areas as critical, due to insufficient reproduction of the real process conditions. Therefore, the illustration accuracy is enhanced through a variety of different arrangements.

2.1. Material experiments and material model

The part is made out of DC06 steel. In AutoForm predefined material cards can be used for simulations, which are an average of different batches and suppliers. To achieve the best accuracy possible of the material model, several experiments with the specific material used for the trunk lid were done. From this data an optimized material was generated and used in the simulations. The characteristic flow behaviour of the material is measured by doing tensile experiments in rolling direction of the material. The anisotropy coefficient, yield stress, tensile strength and equivalent strain are measured in 0°, 45° and 90° to rolling direction with additional tensile experiments.

The tool temperature is increasing monotonously during the serial pressing. Depending on the part, part number and measuring point, large temperature differences can be observed. Hence, the material behaviour is measured between 20°C and a maximal temperature of 80°C in steps of 20°C.

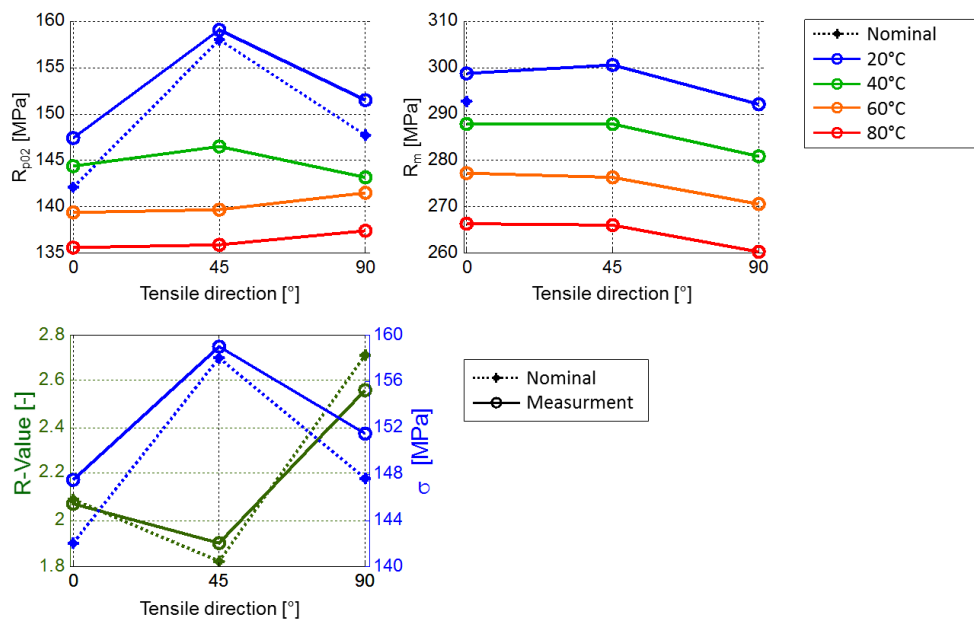


Figure 1: Measured material coefficients at different temperatures

The yield stress shown in figure 1 above decreases in average of about 5 MPa with a temperature increase of around 20°C. Except the yield stress in 45° tensile direction at room temperature decreases much faster for higher temperatures, which implies a decreasing anisotropy. However, the measurement of the yield stress is quite sensitive in evaluation, although the values are averaged over three experiments. Thus, the interpretations of the absolute values have to be taken with caution. On the other hand the tensile strength is quite robust in evaluation. In each tensile direction the tensile strength drops down about 10 to 11 MPa per temperature increase. The reduction of the tensile strength is about twice of the yield stress. Consequently the growth of tension through hardening declines with increasing temperature. In other words the material holds out less and therefore has a worse formability. The comparison between the anisotropy coefficients (R-values) from the nominal values of the supplied material data sheet and the measured R-values at 20°C shows quite similar values. The differences are all in the range of variation of changing coils. Also the differences in yield stress between the nominal

data and the measured data result from the fluctuation between the coils. The deviations of the individual experimental values to the averaged values (averaged values are shown in figure 1 and figure 3a) are all in the range of 1.5%.

By using a Bulge-Test the biaxial stress is evaluated. Furthermore, the Bulge-Test is used to enhance the prediction of the flow behaviour at strains greater than the equivalent strain. By means of the principle of equivalent work the biaxial stress state is transformed into a uniaxial stress state [6] (see figure 2). The transformation of the curve is based on the evaluated ratios of σ_b/σ_0 and $\varepsilon_b/\varepsilon_0$ [3]. For the extrapolation range the last values are used.

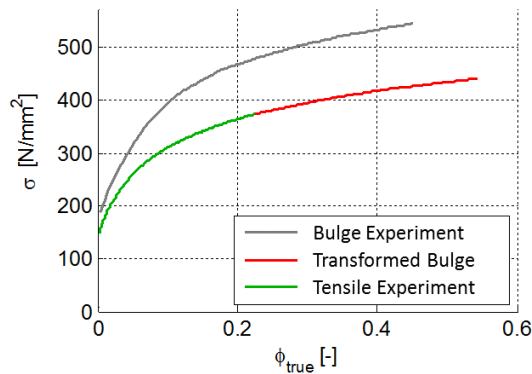


Figure 2: Transformed Bulge curve to uniaxial stress state

The Forming Limit Curve (FLC) is measured by doing Nakajima experiments. The experiments are evaluated with the Method of Volk and Hora (Volk 2011b), which is based on the strain rate evolution [4]. The determined values of the experiments with identical specimen width are averaged and connected with each other. If the line is exceeded, localized necking may occur in the sheet metal. A safety margin of about 20 to 25% is deducted from the measured FLC to take uncertainties in measurement and material deviations into account.

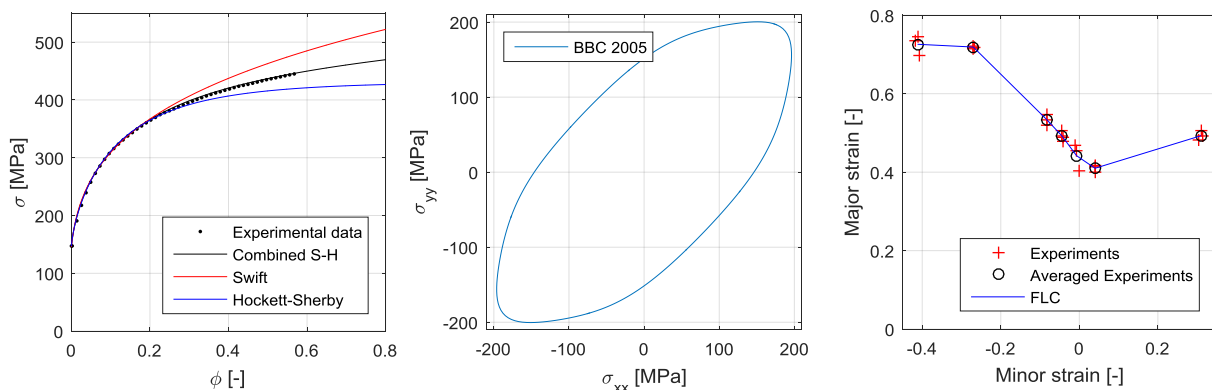


Figure 3: Experimental and fitted flow curve (a), yield locus (b) and FLC (c)

The material model is then created with the AutoForm Material Generator R3.1. The hardening behaviour is fitted at 20°C with the combined S-H approach [8]. The yield locus is fitted with the BBC model for the measured data at 20°C. The biaxial r-value ($r_b = 0.809$) and the biaxial stress ($\sigma_b = 187.9 \text{ MPa}$) are measured in the Bulge experiment.

2.2. Press construction

Most of the major quality problems such as splits, wrinkles, sink marks and skid impact lines occur in the first press operation. Therefore, the press description is restricted to the deep drawing operation.

The mechanical, single-acting press can be controlled over four die cushion forces. To transfer the forces from the die cushions to the binder, 15 cushion quills are arranged symmetrically on each of the four die cushion. For the simulative illustration the forces are reduced from the 15 cushion quills to the corresponding die cushion. This can be calculated with the mechanical equilibrium condition (1).

$$(x_s|y_s) = \frac{\sum_{p=1}^n (x_p|y_p) * F_p}{\sum_{p=1}^n F_p} \quad (1)$$

Hence, four coordinates of force application result for the hydraulic four-point drawing cushion (see figure 4).

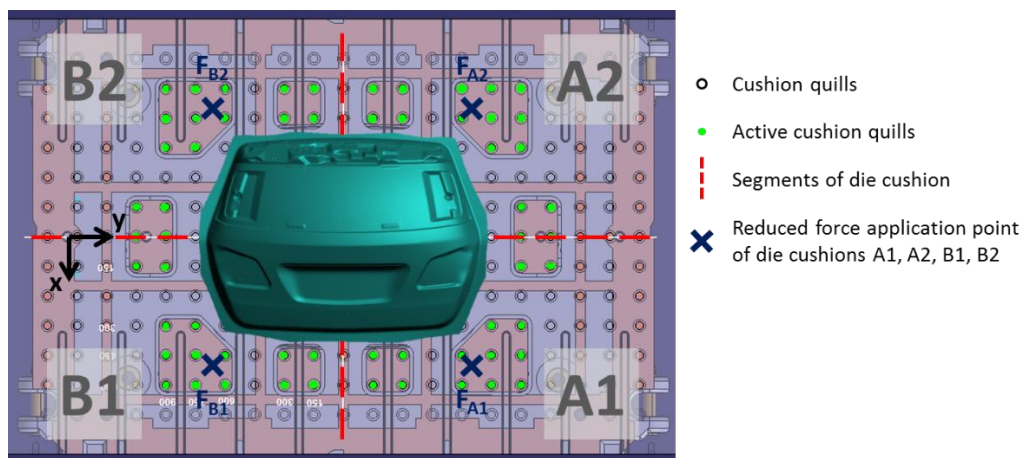


Figure 4: Binder suspension on cushion quills and segments of die cushion

As in the state of the art, which is also implemented in AutoForm, the tools are assumed to be rigid bodies. Therefore, the deflection of any tool is locked. If a certain flexibility is required, a tool stiffness factor can be defined which allows a local homogenisation of the pressure distribution [8]. Because of the equilibrium condition all acting forces can be reduced to one total force with one specific force application point respectively coordinates. This simplification does not influence the simulation result. However, in reality major differences would appear because of the deflection, in particular for large tools. The total force and the coordinates of the binder can be implemented in AutoForm with the function *Columns (User def.)*. In case of the trunk lid, y-coordinate can be neglected because of symmetry. So the x-coordinate and the total force remain.

2.3. Tool geometries

The designed tool geometries of the method plan are used as a reference for the milling geometry. Additionally to the designed geometry, drawbead contours are added to the reference. After milling, the geometries have to be processed by hand in tool tryout to rework the tool regions where splits, wrinkles, sink marks or skid impact lines occur. Thereby, originally designed radii in the punch and in the die are harmonised or increased. Furthermore, most of the efforts are put into the tryout of drawbeads to adjust the draw-in of the blank. Typically the tryout is done in many loops. After each loop the influences of the made adjustments on the part quality are checked in the tryout press.

The simulation of a part with digitised tool geometries strongly differs from the simulation coming from the method plan with exact the same simulation settings. Hence, the tools are digitised after the first tryout loop. Thus, the major problems are remedied, but the complex fine-tuning is still pending.

The digitalization is made with a GOM ATOS measurement system. The finalized and re-meshed geometries have a tolerance of maximum 10 microns.

3. Finding the operating point

The metamodels, which describe the simulation behaviour in terms of different process fluctuations and process settings, should be evaluated around a suitable operating point. First of all, this point is required. It can be found by optimising all parameters of process design, such as binder forces or blank position. The remaining parameters of process fluctuation such as friction and material properties as well as the design parameters will be varied around the selected point.

The suitable configuration of the process design parameters is optimised with a design of experiments. The parameters are the total binder force, the x-coordinate of the force application point (to allow different force distributions), the force on the die inlet and the x-coordinate of the blank position. The die contains a die inlet to avoid skid impact lines. The y-coordinates of the force application point and the blank position stay constant because of the symmetry. Thereby, the four design variables are varied independently over 30 simulations.

The simulation results are then exported from AutoForm and imported into Matlab. Then the critical quality criteria are selected by specifying a result variable and the corresponding region of the criterion. For each defined quality criterion a metamodel is evaluated. Each quality criterion is limited by a specified value, e.g. *Max. Failure* in AutoForm (ratio between the simulated major strain and the major strain from FLC for a given minor strain [8]) at 0.8 or *Thinning* at 2%. By keeping the blank position and the die inlet force constant at a certain value, the contour lines of the metamodels at the specified values can then be visualized in the plane “total force – force distribution”.

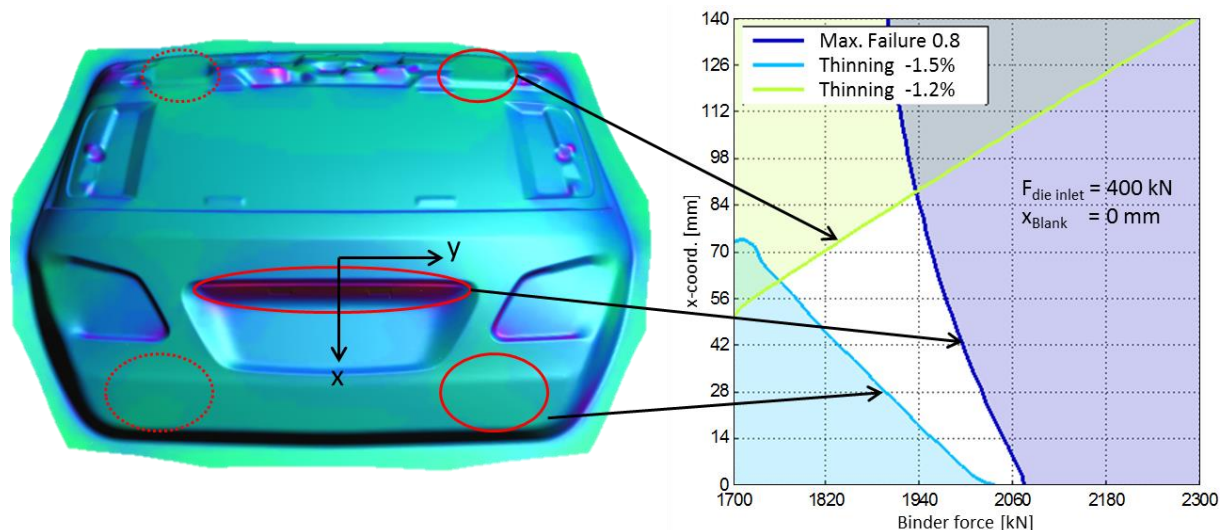


Figure 5: Definition of quality criteria (a) and their process limit in the process window (b)

The coloured regions in figure 5 (b) show the area where the limit of the corresponding quality criteria is exceeded. The remaining white triangle represents the valid process window. A reduction of the force on the die inlet would extend the process window considering the three quality criteria. At the same time the skid impact line is getting worse. Therefore, the force on the die inlet is reduced as much as possible without getting skid impact lines. The determined force is 400 kN. The blank position is then also optimised to enlarge the process window. The best parameter configuration is reached for the initial blank position at 0 mm. The resulting process window for the constant blank position at 0 mm and the constant die inlet force at 400 kN is shown in figure 5 (b).

4. Virtual tryout map

Once the operating point of the simulation with digitised tool geometries is found, a new design of experiment considering the major process fluctuations and the process settings is created. It contains the variation of six independent and three dependent variables, which are shown in Table 1. The total binder

force is deliberately varied for higher forces because the drawbeads are tending to be reduced which results in less critical risk of splits and at the same time in lower thinning in the critical regions shown before. Additionally, lower forces on the die inlet, which is also varied in the new design of experiment, lead to the same effects. The x-coordinate of the force application point (similar to a force ratio) is again varied in a range of 140 mm. However, to optimise the prediction behaviour the centre of the range is moved to the level of the chosen operating point, which leads in a minimum value of minus 60 mm and a maximum value of 80 mm. The friction coefficient reflects the influence of the tool temperature. At the beginning of the serial pressing the tools are cold, which results in lower friction coefficients (nominal value). During serial pressing, the tools are heating up and will reach a steady state value after a certain number of parts. Due to the increasing temperature the lubricant changes its physical behaviour (particularly the viscosity), resulting in an increased friction coefficient [10].

The variations of the material parameters have been measured from ten different batches of material. The measured minimum and maximum of the material coefficients have been taken as upper and lower variation values respectively. It is assumed that the ratios between the r-values (r_0 , r_{45} , r_{90}) as well as the ratios between the yield stress and the tensile strength stay constant (see figure 6).

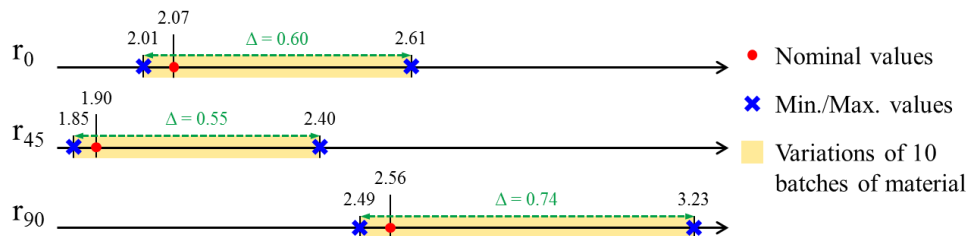


Figure 6: Variations of measured r-values

Table 1: Variation parameters and variation boundaries

Variation parameter	Dependence	Minimum	Maximum
Binder force F_{tot}	Independent	1800 kN	2400 kN
Force distribution x_{Pos}	Independent	-60 mm	80 mm
Force on die inlet $F_{\text{die inlet}}$	Independent	0 kN	400 kN
Friction μ	Independent	0.10	0.16
Yield stress R_{p02}	Independent	137.7 MPa	151.5 MPa
└ Tensile strength R_m	Dependent from R_{p02}	270.6 MPa	310.4 MPa
R-value r_0	Independent	2.01	2.61
└ R-value r_{45}	Dependent from r_0	1.85	2.40
└ R-value r_{90}	Dependent from r_0	2.49	3.23

A quadratic metamodel based on the six influence variables is fitted with 13 parameters. Therefore, 32 simulations are carried out with a Latin-Hypercube-Design to avoid over-fitting and to allow a cross-validation of the metamodels. For each quality criterion, which already have been defined in figure 5 (a), a metamodel is calculated and validated with the leave-one-out cross validation method. Furthermore, the influences of the varied parameters on the defined quality criteria are quantified by using a sensitivity analysis. For this the FAST-method (*Fourier Amplitude Sensitivity Test*) is applied. Figure 7 shows the percentage of the sensitivities on the AutoForm criteria *Max. Failure* (license plate) and *Thinning* (spoiler region). The remaining quality criteria based on Thinning demonstrate a very similar behaviour as the criterion in figure 7 (b).

The calculated sensitivities are directly related to the variation range of the parameters. Therefore, the upper and lower variation values of the forces are based on the typical press settings during a serial

pressing and the lubrication values are based on experience values [7]. The sensitivities for *Max. Failure* (around the license plate) in figure 7 (a) suggest that an increasing friction, due to rising tool temperature during serial pressing, cannot only be corrected by a reduction or a redistribution of the forces to stabilise the process. For this reason the influences of the forces seem to be too small in comparison to the friction. This leads to an increasing risk of splits. One of the possible relieving actions is using a higher amount of lubrication as it is confirmed in the real process behaviour, whereby higher costs are the consequence [9]. For *Thinning* criteria, friction is also the most influential variable. The influences of the forces are in total 36%, so that changing friction behaviour can be partially corrected only by adjusting the press forces. The identified actions are restricted to local behaviours. Therefore, they could influence the part globally, wherefore it is necessary to analyse the effects separately.

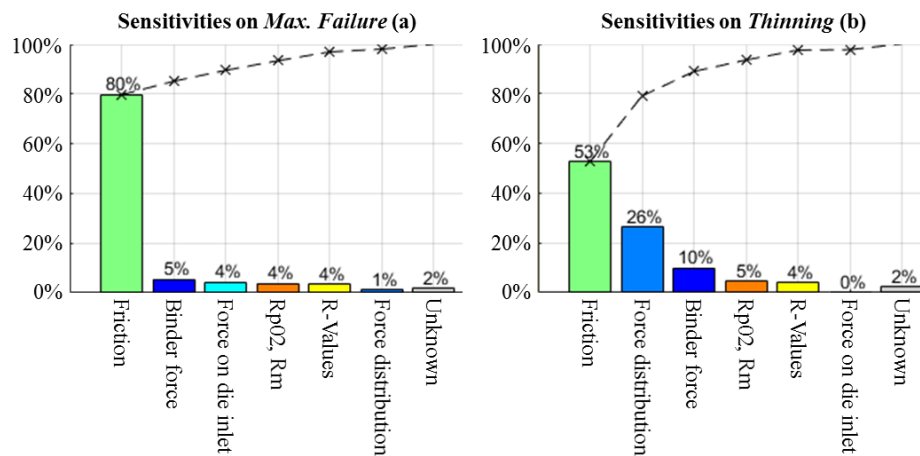


Figure 7: Sensitivities on *Max. Failure* (a) and *Thinning* (b)

Furthermore, correlations are calculated between the draw-in and the different quality criteria defined in chapter 3. For this the draw-in values of each simulation of the design of experiments are correlated with the simulation results of the predefined quality criteria. Each draw-in point on the contour around the part in figure 8 represents a vector of draw-in results of the 32 simulations. Also each quality criterion has 32 results from the different simulations. The draw-in values for each point around the part are correlated with the respective quality criteria and coloured depending on the resulting correlation value (see Figure 8).

$$\left. \begin{array}{l} \text{Draw-in lengths for point } i: \\ (n \text{ simulations}) \end{array} \right\} l_i = \begin{bmatrix} l_{i,1} \\ l_{i,2} \\ \vdots \\ l_{i,n} \end{bmatrix} \\
 \left. \begin{array}{l} \text{Values of quality criterion } q: \\ (n \text{ simulations}) \end{array} \right\} v_q = \begin{bmatrix} v_{q,1} \\ v_{q,2} \\ \vdots \\ v_{q,n} \end{bmatrix}$$

Correlation: $c_{q,i} = \text{corr}(l_i, v_q)$

- For each quality criterion q correlation values c_q are calculated.
- Each entry of the correlation array describes the correlation of the draw-in at one point i of the part boundary.

This procedure is done exemplarily for the two quality criteria, *Max. Failure* and *Thinning* in the lower part region (see figure 5). The coloured contour is located on the part boundary in the undeformed stage right after closing the binder with the die. The gap between the correlation points and the deformed part boundary (grey) depicts to the draw-in of the part.

The draw-in correlations detected to be relevant for the *Max. Failure* criterion in the middle of the part are surprisingly not as expected in the lower part region (see figure 8 a). The draw-in correlating the best with the risk of splits in this region is located sideways of the part (circled in blue). For the

Thinning criterion the best correlations occur in the lower part boundary. The correlation values are nearly symmetric because of the intrinsic symmetry of the part and the fact that the force distribution is only varied in direction of x-axis.

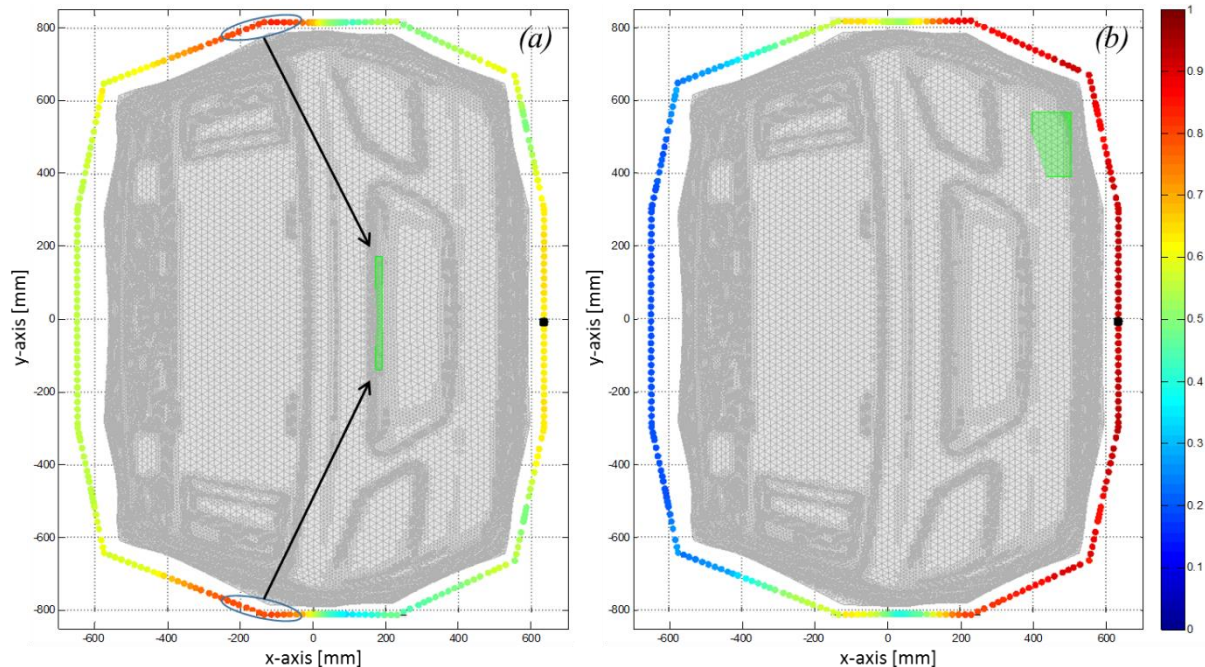


Figure 8: Draw-in correlations with Max. Failure (a) and Thinning (b) criteria

The identified draw-in regions are supposed to be the relevant drawbeads, which have to be reduced (or intensified) to improve the quality of the part in the corresponding quality criterion. In some cases a reduction of a drawbead is not only improving a quality criterion, but it can also deteriorate another. To avoid this effect all relevant correlations (values over 0.75) are determined and transferred into one global tryout map (see figure 9). In case the superimposition shows overlapping segments the workforce of the tool tryout is warned to change these drawbeads with caution. For the presented part example no overlapping influences could be detected. Therefore, the three quality criteria can be worked in separately. Instead of intensifying the drawbeads for the two *Thinning / Insufficient Stretch* criteria by welding, the binder force could be increased and in return the sensitive drawbeads to the Max. Failure criterion (bordered in green) could be reduced.

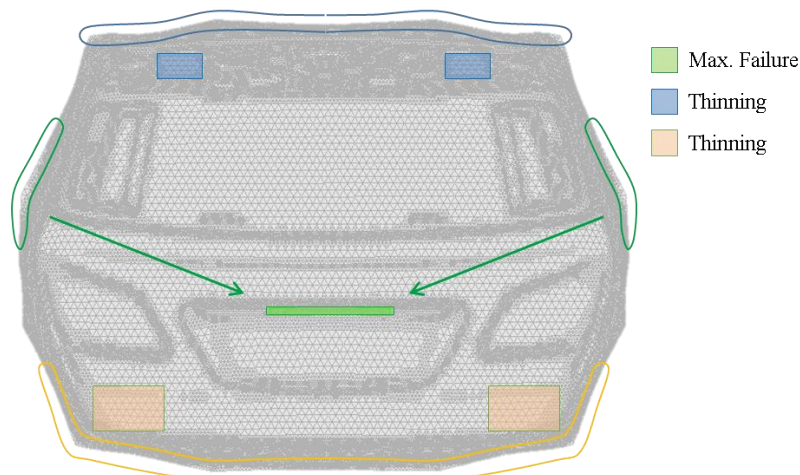


Figure 9: Superimposition of draw-in correlations result in tryout map

The developed methodological approach of virtual tryout planning has been compared with the real tryout steps that have been done on the presented tool. A very good accordance between the virtual tryout and the real behaviour of the part could be determined [9].

Moreover, the virtual draw-in correlations are very useful to identify the position of a sensor, which is relevant enough to observe the process or in particular the accordant quality criterion. Such a sensor is able to quantify a potential split, wrinkles or insufficient stretch, depending on where the sensor is positioned. In serial production the quality of the part is identified after the last step of the transfer press.

5. Conclusion and Outlook

The simulative agreement with the real process condition is essential to judge quality criteria. Already small simulative changes, such as appropriate material modelling and the force transmission of the binder, contribute significantly to a proper reproduction of the behaviour. The virtual drawbead models used in the die face engineering are sufficient to evaluate the feasibility of the process and to detect the potential critical zones in the part. To obtain more accurate information about the part, to show realistic process windows and to generate virtual tryout maps, the tool geometries used in simulation have to be digitised. Because these tool geometries display the modifications and tryout effects done so far on the surfaces. Especially the draw-in is mapped much better, if real drawbead geometries are used in comparison to the virtual drawbead models implemented in AutoForm.

The virtual draw-in correlations allow the illustration of tryout maps and the transfer of the virtual process understanding to the tool tryout workforce. Thus, the tool tryout will not be based on personal experience of the workforce but on a methodological approach. The comparison between the virtual determined measures and the real performed tryout steps has shown a very good accordance with the results. By means of the performed analyses and developed illustrations, tool optimisations in the methodology planning and in tool tryout can be shortened. Moreover, the amount of scrap parts can be reduced due to more robust process design.

The determined correlations between draw-in and quality criteria are particularly useful for the assessment of the process observation of a subsequent process control. The presentation of the correlations around the part in colour show immediately where a draw-in sensor should be positioned, which is significant enough, to evaluate a quality criterion qualitatively. Therewith, based on a few draw-in and the deposited metamodels, a process control can be realised. In case the draw-in differs from original condition the controller reacts and regulates the process back into the valid operating point.

References

- [1] D. Hortig. *Experiences with the Robustness of sheet metal forming processes*. Forming Technology Forum 2011, Proceedings, Zürich, 2011.
- [2] P. Hora, J. Heingärtner, N. Manopulo, L. Tong. *On the way from an Ideal Virtual Process to the Modelling of the Real Stochastic*. Forming Technology Forum 2011, Proceedings, Zürich, 2011.
- [3] P. Hora, B. Hochholdinger, A. Mutrux, L. Tong; *Modeling of anisotropic hardening behavior based on Barlat 2000 yield locus description*; FTF 2009
- [4] W. Volk, P. Hora. *New algorithm for a robust user-independent evaluation of beginning instability for the experimental FLC determination*. International Journal of Material Forming, Volume 4, Issue 3, pp 339-346, 2011.
- [5] C. Annen. *Entwicklung einer neuen Methode zur Ermittlung und Visualisierung von robusten Prozessfenstern in der Blechumformung*. Diss. ETH Nr. 20573, ISBN 978-3-906031-35-4, 2012.
- [6] P. Peters. *Yield functions taking into account anisotropic hardening effects for an improved virtual representation of deep drawing processes*. Diss. ETH Nr. 22707, 2015.
- [7] J. Krauer. *Erweiterte Werkstoffmodelle zur Beschreibung des thermischen Umformverhaltens metastabiler Stähle*. Diss. ETH Nr. 19070, ISBN 978-3-18-367602-6, 2010.
- [8] AutoForm. *Helpviewer 11.5.4*. AutoForm Engineering GmbH, Version AutoForm R3.1, 2011.

- [9] N. Schelhammer, Mercedes-Benz Cars Operation – Press line 3 & 4 (TF/PW4), Sindelfingen; *Private communications*, 2014.
- [10] H. Watter. *Hydraulik und Pneumatik*. Springer Link, ISBN 978-3-658-01310-3, 2013.